INT. J. RADIAT. BIOL 1997, VOL. 72, NO. 4, 375–385

A charged-particle microbeam: I. Development of an experimental system for targeting cells individually with counted particles

M. FOLKARD*, B. VOJNOVIC, K. M. PRISE, A. G. BOWEY, R. J. LOCKE, G. SCHETTINO† and B. D. MICHAEL

(Received 17 January 1997; accepted 17 June 1997)

Abstract. Charged-particle microbeams provide a unique opportunity to control precisely, the dose to individual cells and the localization of dose within the cell. The Gray Laboratory is now routinely operating a charged-particle microbeam capable of delivering targeted and counted particles to individual cells, at a dose-rate sufficient to permit a number of single-cell assays of radiation damage to be implemented. By this means, it is possible to study a number of important radiobiological processes in ways that cannot be achieved using conventional methods. This report describes the rationale, development and current capabilities of the Gray Laboratory microbeam.

1. Introduction

A microbeam is a source of focused or collimated radiation localized to a micron-sized area (or thereabouts) of the specimen. Charged-particle microbeams are most often used for high spatial resolution quantitative analysis of geological, historical or biological samples. The development and use of microbeams as an analytical probe is described in detail by Watt and Grime (1987). Until recently, there has been very little active research using microbeams of ionizing radiation for radiobiological applications, although it is interesting to note that one of the first applications of a charged-particle microbeam was to study the fidelity of cell division following the irradiation of cells in metaphase (Zirkle and Bloom, 1953, Bloom, 1959).

In recent years there has been a resurgence of interest in the use of microbeams in radiation biology. Several groups in Europe, the USA and Japan are developing, or planning to develop an installation for the micro-irradiation of cells *in vitro* using charged-particles (Geard *et al.* 1991, Braby 1992, Folkard *et al.* 1995, Nelson *et al.* 1996). These groups have recognized that it is possible to study a number of important radiobiological processes in ways that cannot be achieved using conventional 'broad-field' exposures. The current interest in micro-irradiation techniques is timely, as modern facilities will benefit considerably from some of the technological advances that have occurred in recent years (for example, the use of computers in imaging, control of instrumentation and data acquisition systems). Furthermore, a number of recently developed or established biological assays of radiation damage are now sensitive enough to be used at low doses, where microbeams will have a critical role.

This publication is the first of a series to report on the design, implementation and use of the Gray Laboratory charged-particle microbeam. Part I discusses the rationale for developing a microbeam facility, the required specifications to usefully address questions that arise from the rationale and the strategies used to meet these specifications. Part II will consider the development of the particle collimation and detection system, and future publications will report the results of targeted cell experiments using the microbeam and single-cell assays of radiation damage.

2. Rationale for the microbeam

The use of a charged-particle microbeam provides a unique opportunity to control precisely, the number of particles traversing individual cells and the localization of dose within the cell. This approach is now seen as one of the primary experimental strategies for investigating the cellular basis of hazards associated with occupational and environmental exposure to low doses of charged particles. For example, the exposure to low levels of naturally occurring radioactive radon gas (and its daughters) amongst the general population is known to be widespread (Brenner *et al.* 1995). At the levels of dose that generally apply in these circumstances, virtually no cell receives more than one charged-particle traversal in its lifetime and neither epidemiological studies of high risk groups such as Japanese bomb survivors and uranium miners, nor conventional *in vitro* cell experiments (i.e. using an un-collimated 'broad-field' irradiator, see Folkard *et al.* 1996) can readily address this point. By contrast, the charged-particle microbeam is ideally

*Author for correspondence.
Gray Laboratory Cancer Research Trust, PO Box 100, Mount Vernon Hospital, Northwood, Middlesex, HA6 2JR, UK.
†King's College London, Strand, London WC2R 2LS, UK.

0955–3002/97 $12.00

suited to developing an *in vitro* experimental model for reproducing the levels of exposure that occur *in vivo*.

The microbeam will be useful in addressing observations related to cellular spatial sensitivity. For example, it is known that an average of about 2–5 α-particle traversals are required to kill a cell. Each particle crossing the nucleus will (in theory) intersect the DNA many times and it is unclear how some cells are able to survive this. In a study by Raju and colleagues (Raju *et al.* 1991), it was shown that α-particles which completely traverse the nucleus are more effective per unit average dose, than those terminating within it. This finding differs from the earlier work of Cole and co workers (Cole *et al.* 1980) who showed that the DNA close to the nuclear membrane is the most easily damaged by ionizing radiation. A microbeam with sufficient resolution could be used to gain further insight into the true nature of cellular spatial sensitivity.

There have been several reports that radiation effects may be transmitted from irradiated cells to neighbouring un-irradiated cells. Nagasawa and Little (1992) found an unexpectedly high frequency of sister chromatid exchanges following exposure to doses of particles low enough that only a fraction of the cells are hit. A similar finding is reported by Deshpande *et al.* (1996) who demonstrated that α-particles, can induce sister-chromatid exchanges without directly traversing cell nuclei. Hickman *et al.* (1994) reported the expression of wild type p53 protein (believed to have a critical role in maintaining genome integrity following radiation damage) greater than would be expected following low doses of particles. A microbeam facility can be used to selectively irradiate individual cells which can be subsequently re-visited to ascertain what changes have occurred to that cell, and to its un-irradiated neighbours.

Although the action of ionizing radiations has been closely linked to the way it damages DNA, there is increasing interest in other pathways of damage and cell death. It has been proposed that apoptotic cell death can be triggered by mechanisms other than damage to the DNA, for example, by damage to the cellular membranes (Haimovitz-Friedman *et al.* 1994). Using the microprobe, this study proposes to look for pathways, other than DNA damage, that may trigger apoptosis.

3. Methods

3.1. *Design criteria*

Outlined below are a number of basic operational criteria for the microbeam that were, *at the time of inception*, considered to be both necessary and achievable using current technology. For experiments where the only criterion is for the particle to traverse the nucleus, then the overall spatial accuracy can be of the order of $\sim 5\,\mu$m (for instance, if the target is the nucleus of a V79 cell). If however, one wishes to target the cytoplasm, or localize dose (as far as possible) to the nuclear membrane, then more stringent demands apply; an accuracy approaching 1 μm is appropriate in these circumstances. To fully exploit the collimator performance, the sample alignment accuracy, the particle beam 'aiming' accuracy and sample image spatial resolution should match the collimator resolution. An efficient particle detection and beam shuttering arrangement is necessary to study the effects of single-particle or pre-selected multiple-particle traversals. The delivery of the correct number of particles in $<95\%$ of individual exposures was considered necessary. Finally, it is important that the process of target identification, alignment and irradiation are both automated and rapid, so that the time to irradiate a statistically significant number of cells is not unduly long. A cell throughput (during the irradiation phase) of about 1 cell s^{-1} is desirable.

3.2. *Particle delivery*

A general view of the installation is depicted in Figure 1. The microbeam utilized the Gray Laboratory 4 MV Van de Graaff accelerator, which could accelerate singly- or doubly-charged particles, generated using a radio-frequency ion source. Accelerated particles of the desired mass and energy were selected using an analysing magnet which bends the vertical particle beam into a 4 m horizontal section of beamline. Along the beamline was an arrangement of slits, quadrupole magnets and electrostatic steerers, used to define the beam profile and trajectory. The horizontal beamline transported the particles into an experimental room used routinely for a variety of charged-particle and neutron-related studies. The microbeam facility was installed in a room directly above this area by extending the charged-particle beamline 3 m vertically upward. As a consequence, the existing experimental area remained relatively undisturbed and the microbeam was in the optimum orientation for ease of use (i.e. vertically upward). Another benefit was that the floor of the microbeam room (through which the beamline passes) was formed from 1·5 m thick concrete and was an excellent platform on which to support the microbeam, such that no special measures were required to isolate the irradiation stage against vibration.

Once in the microbeam room, the particle beam passed through an isolating vacuum gate valve, into a 1 m long by 16 mm diameter section that incorporated two sets of micro-adjustable slits (arranged

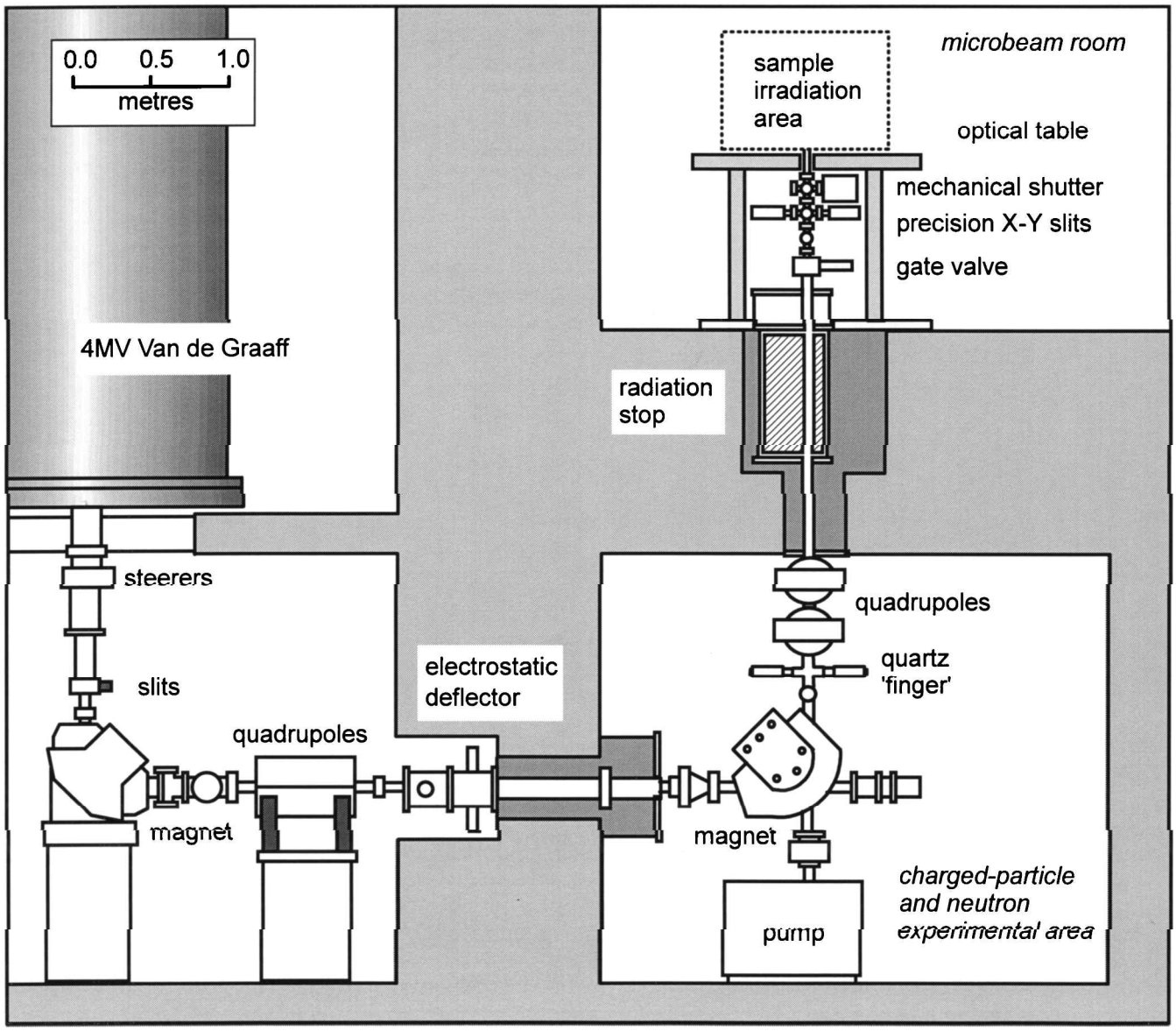

Figure 1. The Gray Laboratory Van de Graaff beamline.

orthogonally) and a mechanical shutter. Finally the beamline passed through the centre of a 1·25 m by 1 m optical table at bench height and was terminated by the micro-collimator. The optical table was used to support the sample irradiation stage, and the imaging system. The micro-adjustable slits pre-collimated the beam to an area of a 1–3 mm^2 and served primarily as an indication that the beam was correctly aligned. Each slit jaw was connected to an electrometer, such that the current readings could be used to centre the beam.

3.3. *The collimation and detection system*

Details of the particle collimation and detection system are considered in detail in a separate paper. Briefly, the current collimator was made from 245 μm diameter by 1 mm long glass capillary with either a 5 μm, 1·5 μm or 1·0 μm diameter bore. This was 'capped' at the exit by a 3 μm Mylar vacuum window and an 18 μm thick scintillating film through which the particles passed. During the irradiation sequence, a photomultiplier (PM) tube, above the cell dish, detected photons that were generated in the scintillator by the passage of a charged-particle.

3.4. *The sample irradiation stage*

A schematic diagram of the sample irradiation stage is shown in Figure 2. The system was designed to irradiate mammalian cells (in the first instance,

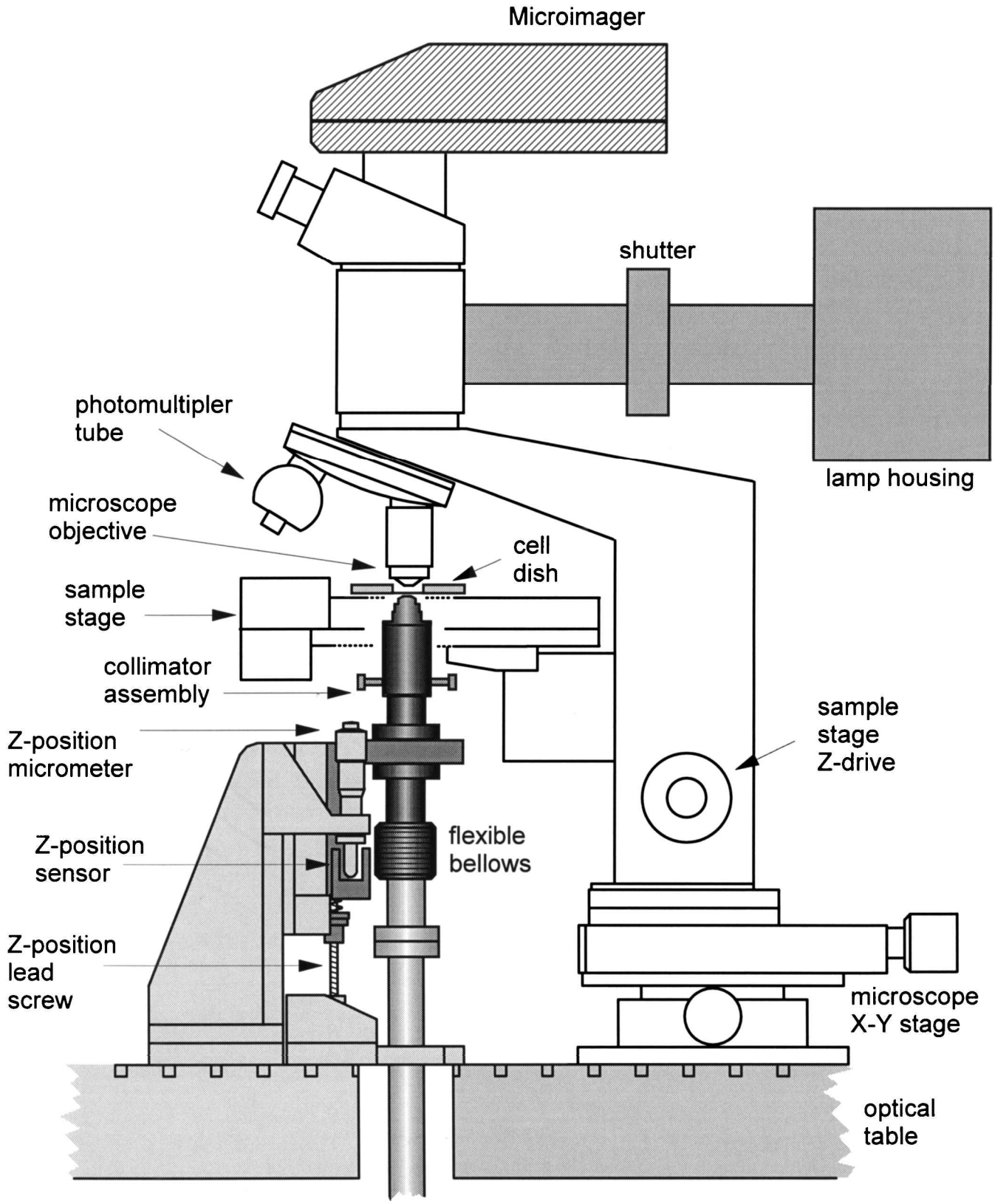

Figure 2. The sample irradiation stage showing the arrangement for aligning the cells and the collimator, and for imaging the cells.

V79-379A Chinese hamster cells) attached to a thin membrane that formed the base of a cell dish (see section 3•7). The dish was supported on a motorized X–Y microscope stage (Märzhäuser, Wetzlar, Germany) that was positioned using a stepper-motor coupled leadscrew (with a resolution of 250 nm/motor microstep) on each axis. The cells could be viewed *in situ* using an epi-fluorescent microscope (Olympus, type BH2), either through the eyepiece, or more usually, with a charge-coupled device (CCD) imaging system (see section 3.5). The sample stage was supported by the focusing mechanism of the microscope, which was also motorized. The action of this mechanism was to move the whole stage vertically (i.e. in the Z-direction) with respect to the collimator and the static objective lens. The microscope was coupled to the optical table by a manually driven X–Y micropositioning stage, which was used to position the whole microscope such that the objective lens was directly above the collimator (so that the collimator exit can be viewed). The procedure for irradiating cells required that the vertical position of the collimator was precisely controlled. To do this, vacuum bellows were installed in the final section of beamline to allow up to 20 mm of vertical movement of the collimator assembly. This was supported by a substantial precision linear ball-slide, that permitted the collimator to be moved vertically up (against atmospheric pressure which is acting to 'squash' the bellows) or down by an action of a DC-motorized lead-screw. The vertical position of the collimator was set precisely by driving the collimator assembly upward until an 'arm' on the side of this assembly came into contact with the adjustable end of a micrometer (this is sensed electronically).

The micro-irradiation of cells required that each cell was aligned, one-by-one, so that the target was immediately above the collimator exit. The microscope was central to this part of the procedure. Before each dish of cells was irradiated, the collimator exit was brought into focus (viewed through the media in the cell dish) using the micrometer arrangement described above, and its X–Y co-ordinates were recorded. The same micrometer was now used to lower the collimator by a small, but known amount (say, 10 μm) such that if a cell was in focus at the recorded collimator position, the collimator would be directly below that cell, just touching the underside of the cell dish. An infrared optical sensor was arranged to detect the collimator position 0•5 mm lower than the irradiation position. The collimator was lowered to this position whenever the stage was moved (i.e. when the next cell is positioned) so that the moving cell dish did not interfere with the collimator. At the beginning and end of an irradiation sequence, the collimator could be lowered a further 20 mm to allow access for inserting or removing the cell dish.

3.5. *The micro-imaging system*

For the majority of planned experiments, it was essential that the cell nucleus was clearly visualized. For this reason, an *in situ* epi-illuminating (either UV or visible light) micro-imaging system arranged to view both the cells and the particle collimator was used. To identify the cell nuclei, cells were stained with a UV-fluorescent dye, such as the DNA-binding dye, Hoechst 33258. There are a number of considerations that arose from this approach; Hoechst 33258 (and other nuclear stains) is known to be radio-modifying at typical working concentrations. Also, viewing the cells under UV illumination can cause unwanted, non-ionizing damage to the cells. To counter these undesirable effects, an imaging system was installed that has a high light sensitivity, without compromising the optical spatial resolution, so that both the dye concentration and the UV dose could be minimized. This system was based on a Xillix Microimager 1400 (Xillix Technologies Corporation, Richmond, Vancouver, Canada) that used a 1•4 Mpixel, uncooled, integrating CCD array (Kodak KAF 1400). A feature of this particular CCD is that the individual pixels are confluent (i.e. no 'dead-space' between pixels, which maximises sensitivity) and are small (7 μm × 7 μm). This permits the use of a low power, ×10 objective but retains good spatial resolution without the need for further optics (which would reduce sensitivity). Under good illumination conditions, and using a ×10 power objective lens, the resolution of the imaging system was ~1 μm.

Further measures were introduced to reduce the UV dose to the cells. A fast mechanical shutter was installed in the UV-excitation light path to operate in unison with a similar device that was part of the micro-imager, such that the sample was illuminated only during the image integration cycle of the micro-imager. Furthermore, the sensitivity of the CCD amplifier was increased by a factor of ×3 greater than its factory setting; although this degraded the dynamic range and black level stability performance to some extent, the imager performance was found to be acceptable and clearly reduced the UV excitation dose by the same extent. Where possible, images were acquired as a single 'snapshot' of approximately 50 ms duration. For 'dynamic' imaging, (for example, when focusing) successive images were acquired at a rate of about 2–4 Hz. Normally, only cells outside the experimental area will be viewed dynamically.

3.6. *Experimental control*

Virtually all operational features of the microbeam were controlled using a 66 MHz, 486 PC. The PC was supplied in the first instance by Xillix (it has been recently upgraded), complete with software for processing images from the micro-imager, and to control the movement of the sample stage in all three planes (via the RS232 port). This software was used as a 'platform' for implementing the image analysis program and experimental automation procedures, and for controlling additional peripheral devices. Figure 3 shows the principle connections between the microbeam and its PC-based controller.

The CCD image was digitized (12 bit) and transferred to a Matrox 1280 image processing board installed within the PC and was displayed on a 1280×1024 pixel monitor. The same board also generated signals to energize the leaf-shutters on the imager and the UV excitation lamp. The PC supports a card with an IEEE 488 interface, which was used to communicate with a number of custom-built experimental control modules, installed within a single 48 cm rack. One module was dedicated to sensing and moving the collimator to one of three possible positions in response to commands, either from the PC, or from a manual control. Other modules provided pulse-shaped amplification, pulse-height discrimination and (if required) coincidence for two independent charge pre-amplifier detector signals. As an aid to beam alignment, a simple ratemeter module can be used to display the intensity of 'continuous' beams. A 3-digit display shows accumulate counts from the detector, and could be preset to terminate the exposure of each cell when the desired counts were reached. Irradiations are terminated by the action of two shutters, controlled by another module within the rack. Rapid exposure termination was achieved using an electrostatic shutter sited midway between the two 90° bending magnets to deflect the beam. This deflector power

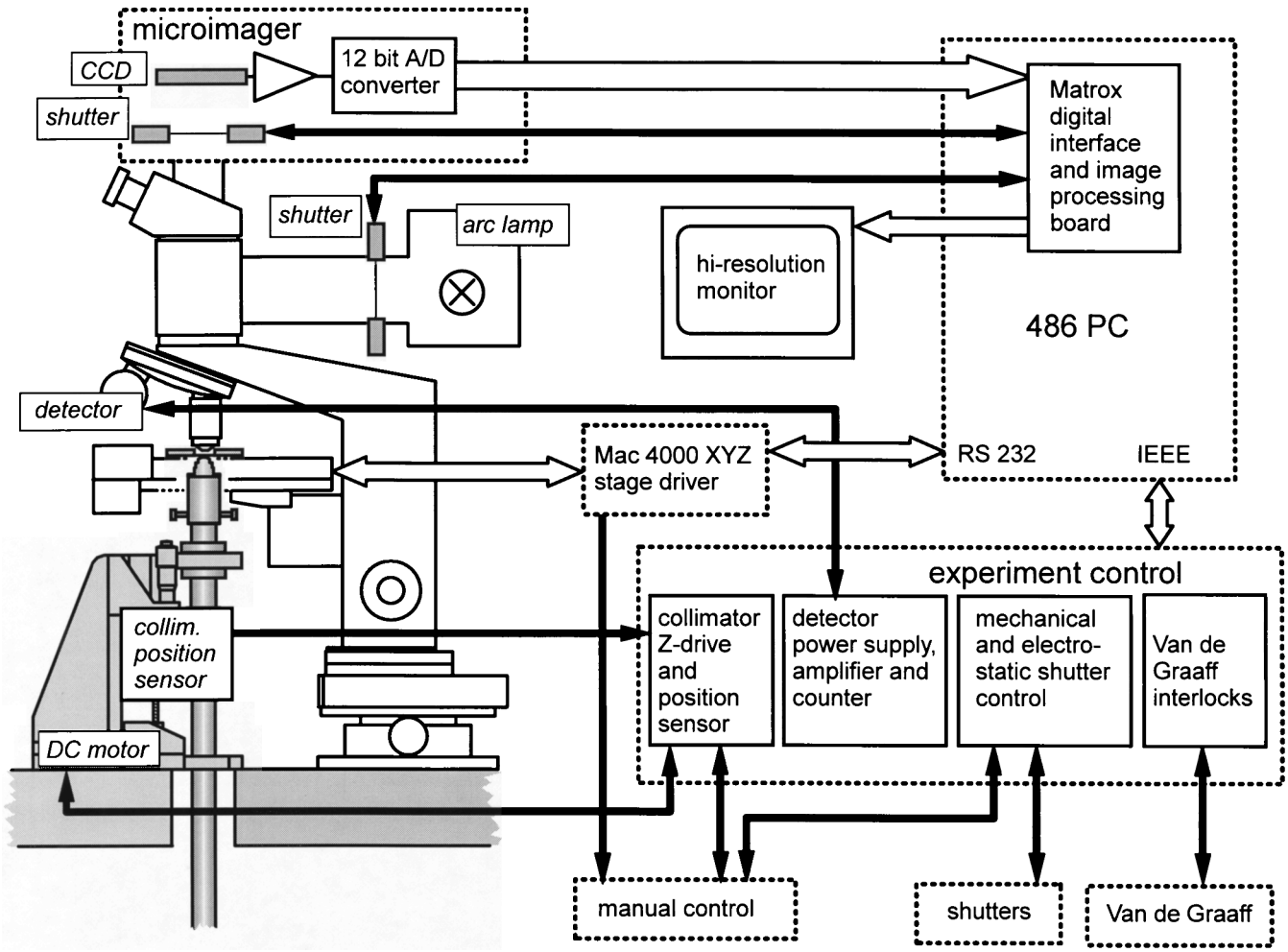

Figure 3. The principle connections between the microbeam and its PC-based controller.

supply generated 250 V mm^{-1} in a few microseconds, but was sustainable for only 50 ms. Within the brief period that the beam was deflected out of alignment, a solenoid operated mechanical shutter was energized to provide a sustained 'beam-off' condition. Finally, there was a module that monitored and displayed the current on the micro-adjustable slits. This information (and other relevant data) was relayed to the Van de Graaff accelerator control console during the experiment.

3.7. *Design of the cell dish*

The design of the dish for supporting the cells had to satisfy the particular requirements of the microbeam; in particular, cells had to be attached to a thin membrane (optically transparent, and non-UV fluorescent), such that there was good access from both sides of the dish for the collimator, the detector and for viewing. Another consideration was the ease of construction, since it was usual to use each membrane once only. Figure 4 depicts a section through an assembled cell dish. The dishes were machined from medical-grade stainless steel. The 115 mm square dish base was designed to register positively with a clamping arrangement on the micro-positioning stage. A 34 mm diameter thin membrane cell support (made from 3 μm thick Mylar, or 4 μm thick polypropylene) was 'sandwiched' between the base and an annular piece that tensioned the membrane as it was located. A 0·5 mm thick silicon rubber gasket provided a water-tight seal. Note that the membrane was the lowest part of the dish, which allowed unimpeded access to position the collimator close to any part of the underside of the membrane.

4. The experimental procedure

The routine for micro-irradiating cells can be divided into five distinct phases:

1. Sample preparation;
2. Microbeam initialization;
3. Cell finding;
4. Irradiating the cells; and
5. Assaying for radiation damage.

Each aspect of the irradiation sequence is discussed in detail below.

4.1. *Sample preparation*

Before each experiment, fully assembled cell dishes were sterilized by γ-irradiation (2·5 days at ~10 Gy/min) in sealed containers. Cell dishes either had bases of 3 μm thick Mylar or 4 μm thick polypropylene. For polypropylene-based dishes, Cell-Tak adhesive (Becton-Dickinson, Bedford, MA, USA) was added to these dishes at a final concentration of 2–3 μg/ml for 30 min followed by several washes in sterile water. For Mylar based dishes, these were pre-treated by incubation with cell culture medium for 12 h prior to use. For all cell manipulations, freshly filtered Eagles complete minimal Essential medium (CMEM) supplemented with 10% (v/v) foetal calf serum and penicillin (100 IU/ml) and streptomycin (100 μg/ml) were used. On the day of the experiment, freshly harvested V79-379A Chinese hamster cells were seeded into the dishes at a concentration of around 3×10^3 cells/dish to give a final concentration of 50–200 cells per 25 mm^2 area. Around 1 h before the start of the cell irradiation, Hoechst 33258 was added to a final concentration of 1 μM and incubation continued at 37°C. At the time of irradiation the cell culture medium was removed and gently washed and replaced with HEPES-buffered CMEM to a depth of 0·5 mm in the dish (approximately 0·5 ml). In this arrangement the cells could be viewed from above without the microscope objective dipping into the solution. Cells were imaged using a ×10 objective and UV filter cube giving excitation of 365 nm and

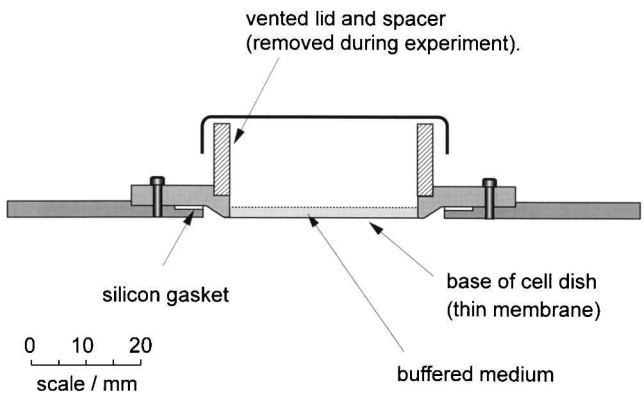

Figure 4. A section through an assembled cell dish.

emission of 420 nm with a typical integration time of 50 ms. Scanning of the dish for cell location, irradiation and revisiting took place at room temperature. After scanning and irradiation, cell dishes were removed from the microscope, fresh CMEM added and replaced in the incubator. Cells were then incubated for various periods of time, depending on the endpoint being scored, before being revisited.

4.2. *Microbeam initialization*

At the start of each experimental day, the collimator was aligned by locating a silicon surface-barrier detector above the collimator and tilting the collimator on a gimballing arrangement until the dose-rate was maximized. At the same time, the energy spectrum measured by this detector was viewed on a calibrated multi-channel analyser to confirm that the collimated particles were near-monoenergetic and of the desired energy. An abnormal spectrum usually indicates that the collimator is mis-aligned or partially blocked (in which case it will be replaced). Once aligned, the particle fluence was adjusted so that about 1–10 particles s^{-1} passed through the collimator. Experience showed that the system will remain aligned for the duration of the experiment, provided that monitor current readings on the micro-adjustable slits (see section 3.2) were maintained.

The sample stage was now initialized and 'registered'. The registration step established the imaging system magnification and the stage co-ordinate system relative to the imager and ensured that cells could be correctly positioned and re-visited at a future date, irrespective of any re-alignment of the stage and the imager. This was achieved by installing and viewing a calibration jig that comprised an opaque rectangle (a microscope reticule) over a fluorescent screen. The collimator position was now established by simply imaging the top of the collimator and using the mouse pointer on the computer screen to place a marker at the collimator exit. This marker remained logged and 'on-screen' for the duration of the experiment.

4.3. *Cell finding*

To locate the cells (and to log their co-ordinates), the cell dish was divided into two, or more regions, depending upon the experiment. Usually, four regions were selected, each 5 mm × 5 mm, arranged over a 11 × 11 mm square area. All cells within two of the regions were irradiated, while the remaining regions served as controls. The control regions were subject to the same experimental protocol as the irradiated regions, apart from the actual particle exposure step. To locate the cells, an automated procedure viewed each region in turn as a series of 80 slightly overlapping 'frames', where each frame was the field-of-view of the microscope (0·85 mm by 0·75 mm, using a ×10 objective). The computer took a 'snapshot' of each frame and conventional image analysis techniques were used to establish the centre of each fluorescent object found. The co-ordinates of each object were logged, along with 17 other parameters (such as perimeter, area, elongation etc.) used to distinguish the cells from other fluorescent objects.

As the cell dish was moved, it was crucial that the cells in the vicinity of the collimator stayed accurately in the focal plane of the microscope objective, both during the cell finding and the irradiation phase. To achieve this, the computer selected three points close to, but outside each region. At each point, the stage X, Y and Z-drives were used to bring a nearby cell into focus over the collimator, and the 'XYZ' co-ordinate was logged. The computer used the three sets of co-ordinates to establish the inclination of the dish, so that as the stage was moved in its X and Y directions, it could make the appropriate Z-adjustment to keep the cells directly above the collimator in the focal plane.

4.4. *Cell irradiation*

Once all the cells within a region had been identified, and their positions logged, the irradiation sequence for that region was initiated. The collimator was viewed through the dish of cells and its height adjusted so that it was a few microns below the focal plane in its highest position (see section 3.4). The objective lens was now replaced with the PM tube (mounted on the microscope turret) used for particle detection and the sample area was enclosed so that it was in darkness. Note that it is not necessary to observe the cells during irradiation, although there is a option to do this if required (i.e. to check that the system is functioning normally). Clearly, the detector was not operational in the arrangement where cells were viewed.

A single computer command commences the irradiation sequence. The logged co-ordinates of the cells were recalled and used to position each cell, in turn, over the collimator (whose position is also logged). For each cell, the collimator Z-drive moved the collimator 0·5 mm upward to the irradiation position, the shutter was opened until the required number of particles were delivered, when it was closed and the collimator returned to its lower position so that the next cell could be manoeuvred over the collimator. When all the cells in a region had

been irradiated, the facility was configured for cell-finding and the next region on the dish was processed. When all four regions had been completed, the dish of cells was removed and prepared for incubation, or other long-term treatment.

5. Discussion

5.1. *Collimator resolution*

Much effort has gone into developing a collimation system that can deliver the 'best possible' accuracy. These are described in a separate publication. Briefly, the current collimator design can confine 96% of particles to within 5 μm radius and 90% of particles to within a 2 μm radius.

5.2. *Counted particle accuracy*

The ability to deliver a single or pre-set number of particles to each cell depends critically on two factors: the detector efficiency and the termination of exposures with sufficient speed. Using a 18 μm thick scintillator, >99% detection efficiency was observed (see accompanying publication for a full treatment of the detector characteristics). Cells can also receive unwanted extra particles if the shutter fails to terminate the exposure quickly enough. The response time of the electrostatic deflector used to end the irradiation of each cell was about 200 μs. For a count-rate of 10 counts s^{-1}, the probability of delivering an extra particle was ~1%. This is higher than might be expected, indicating that the arrival of particles is not random (i.e. there is a tendency for particles to be 'bunched' in time).

5.3. *Cell finding efficiency*

It is the task of the automated cell finding routine to locate and log the positions of all cells (currently, the cell nuclei) in a pre-selected region. The cell finding efficiency is the fraction of cells correctly identified in this way. Just as important is the efficiency with which found objects that are not cells, are excluded.

In practice, there are two reasons why the system may fail to identify a cell correctly; either because it is too faint, or because two or more cells are touching (such that the cells are counted as one object). There are several factors that influence the visibility of a cell: the UV-excitation dose, the fluorescent dye concentration (and uptake), the camera efficiency, electronic (thermal) noise in the camera and a 'noisy' background in the object. As explained in section 3.5, it is important that the UV dose and the dye concentration be minimized as far as possible. This means operating in a situation where cells are just visible. Increasing the camera light detection efficiency makes it possible to lower the UV dose (either by inserting neutral density filters, or by reducing the camera integration time). For this reason, the gain of the CCD camera was increased above the manufacturer's setting to optimize the overall signal-to-noise in the image.

Reducing sources of 'noise' allows the dye concentration to be reduced. Electronic noise can be reduced by using a cooled CCD, though for short integration times (<1 second) this is of limited advantage. The primary source of 'noise' inherent in the image is unwanted fluorescence from the membrane to which the cells are attached. Mylar, although an excellent material in other respects, is significantly fluorescent. Polypropylene (which we now use routinely), is much better in this respect, but requires further treatment before cells attach to its surface. Currently, the system has been optimized such that no cells are 'missed'. Cells are visible using a dye concentration of 1 μM of Hoechst 33258. The UV dose has not been quantified, but corresponds to that from a standard mercury lamp, with a 50% neutral density filter and a 50–100 ms camera integration time (which is also the total UV-exposure time).

5.4. *Cell positioning and re-visiting accuracy*

The accuracy to which cells can be positioned over the collimator should at least match the spatial resolution of the collimator. In the horizontal plane, the stage stepper motors move in 0·25 μm steps such that the *precision* of the stage is about 0·25–0·5 μm. The positioning *accuracy* however, is about 1 μm due to the mechanical tolerance of the lead-screw. For the purposes of re-positioning cells to their logged co-ordinates, it is predominately the *precision* that determines ability to locate cells. Note that anti-backlash measures are applied (i.e. always positioning objects from the same direction) to ensure that this does not adversely affect the stage performance. Overall (considering also, the accuracy to which the cell finding routine assigns co-ordinates to each found object), the measured current positioning accuracy of the stage is ~1–2 μm in the X and Y directions. In the vertical direction, the positioning accuracy is slightly worse (around 2–3 μm), primarily because the cell-dish membrane is not perfectly flat over the experimental region.

It is usually necessary to re-visit cells after an extended period to assess the biological effects of the irradiation. By using the registration plate to ascertain the relative positions of the stage and the CCD imager, it is possible to find cells using the

co-ordinates established during the cell-finding phase, even if the system has been disassembled and re-built in a different alignment. In fact, the greatest source of inaccuracy is the re-location of the cell dish onto the stage. If the cell dish is removed from the stage, an error of about 10 μm is introduced when subsequently re-located. In practice, this is acceptable for assaying purposes, where it is sufficient just to unambiguously identify each cell (cells are normally separated by distances greater than this). Note that the cell dish was not removed from the stage between the cell finding and irradiation phases, where alignment is critical.

5.5. *Throughput of cells*

It is the ability to identify, align and irradiate cells quickly that distinguishes a well specified modern microbeam from its historical counterpart. It is clear that the nature and frequency of radiobiological effects requires that a statistically significant number of cells be assayed (particularly at low doses). The frequency of markers of lethal chromosome damage or cell lethality are typically 0·01–0·04 following say, the traversal of a single proton. Indicators of radiation risk (i.e. assays based on mutation or transformation) are even lower (10^{-4}–10^{-6}).

The time taken to establish the beam conditions, align the collimator and initialize the stage is typically about 1 h. During this time the cell dishes will be seeded with cells and dye will be added to each dish 1 h prior to the anticipated commencement of the cell-finding phase. With the dish located on the stage, one of four regions is selected and the three-point focusing system is used to ascertain the inclination of the cell dish. This takes roughly 5 min. To find cells, the region is automatically raster-scanned as a series of 80 frames, with typically 3–4 cells in each frame. The time taken to process each frame is about 6 s, therefore to find all the cells in a region takes about 4 min. Next, the microscope objective is replaced by the PM tube (simply by changing positions on the microscope turret) and black-out screens are installed. During the irradiation phase of the experiment, it takes about 1·2 s to complete the sequence of actions required to irradiate each cell (i.e. about 5 min to irradiate 250 cells). Overall, to experiment on 1000 cells, spread over 4 regions (i.e. 2 control, and 2 irradiation regions) takes about 50 min. In a typical working day, 4–5 dishes are processed in this way, such that roughly 2500 cells are individually irradiated per day (and an equivalent number of control cells identified). This rate of experimentation is sufficient to establish the dose-response for a variety of assays, within a realistic time-frame.

6. Conclusions

A facility for targeting cells *in vitro* individually with counted particles has been developed at the Gray Laboratory. In the first instance, the system has been configured to irradiate the nuclei of V79 mammalian cells using monoenergetic protons $<$3·5 MeV. The arrangement for locating, aligning and irradiating cells has been optimized for a rapid throughput of cells. Currently, it is possible to irradiate (or sham irradiate) cells individually at a rate of about 1200–1500 cells h^{-1}, which is sufficient to permit a number of single-cell assays of radiation damage to be implemented. Initial studies are using a single-cell clonogenic assay to measure cell survival and the micronucleus assay as an indicator of chromosome damage, with the emphasis on effect at low doses.

Acknowledgements

The financial assistance of the Cancer Research Campaign, the European Commission and the United Kingdom Co-ordinating Committee for Cancer Research is gratefully acknowledged. We are also pleased to acknowledge the substantial input of the Gray Laboratory mechanical and electronic workshops.

References

BLOOM, W., 1959, Cellular responses. *Reviews of Modern Physics*, **31,** 66–71.

BRABY, L. A., 1992, Microbeam studies of the sensitivity of structures within living cells. *Scanning Microscopy*, **6,** 167–175.

BRENNER, D. J., MILLER, R. C., HUANG, Y. and HALL, E. J., 1995, The biological effectiveness of radon-progeny alpha particles. III. Quality factors. *Radiation Research*, **142,** 61–69.

COLE, A., MEYN, R. E., CHEN, R., CORRY, P. M. and HITTLEMAN, W., 1980, Mechanisms of cell injury. In *Radiation Biology in Cancer Research*, edited by R. E. Meyn and H. R. Withers (New York: Raven Press), pp. 33–58.

DESHPANDE, A., GOODWIN, E. H., BAILEY, S. M., MARRONE, B. L. and LEHNERT, B. E., 1996, Alpha-particle-induced sister chromatid exchange in normal lung fibroblasts: evidence for an extranuclear target. *Radiation Research*, **145,** 260–267.

FOLKARD, M., PRISE, K. M., VOJNOVIC, B., NEWMAN, H. C., ROPER, M. J., HOLLIS, K. J. and MICHAEL, B. D., 1995, Conventional and microbeam studies using low-energy charged particles relevant to risk assessment and the mechanisms of radiation action. *Radiation Protection Dosimetry*, **61,** 215–218.

FOLKARD, M., PRISE, K. M., VOJNOVIC, B., NEWMAN, H. C., ROPER, M. J. and MICHAEL, B. D., 1996, Inactivation of V79 cells by low-energy protons, deuterons and helium-3 ions. *International Journal of Radiation Biology*, **69,** 729–738.

GEARD, C. R., BRENNER, D. J., RANDERS-PEHRSON, G. and MARINO, S. A., 1991, Single-particle irradiation of mammalian cells at the Radiological Research Accelerator Facility: induction of chromosomal changes. *Nuclear Instruments and Methods*, **B54,** 411–416.

HAIMOVITZ-FRIEDMAN, A., CHU-CHENG, K., EHLEITER, D., PERSAUD, R. S., MCLOUGHLIN, M. and FUKS, Z., 1994, Ionizing radiation acts on cellular membranes to generate ceramide and initiate apoptosis. *Journal of Experimental Medicine*, **180,** 525–535.

HICKMAN, A. W., JARAMILLO, R. J., LECHNER, J. F. and JOHNSON, N. F., 1994, α-particle-induced p53 expression in a rat lung epithelial cell strain. *Cancer Research*, **54,** 5797–5800.

NAGASAWA, H. and LITTLE, J. B., 1992, Induction of sister chromatid exchanges by extremely low doses of a-particles. *Cancer Research*, **52,** 6394–6396.

NELSON, J. M., BROOKS, A. L., METTING, N. F., KHAN, M. A., BUSCHBOM, R. L., DUNCAN, A., MIICK, R. and BRABY, L. A., 1996, Clastogenic effects of defined numbers of 3.2 MeV alpha particles on individual CHO-K1 cells. *Radiation Research*, **145,** 568–574.

RAJU, M. R., EISEN, Y., CARPENTER, S. and INKRET, W. C., 1991, Radiobiology of alpha particles. III. Cell inactivation by alpha-particle traversals of the cell nucleus. *Radiation Research*, **128,** 204–209.

WATT, F. and GRIME, G. W., 1987, *Principles and Applications of High Energy Ion Microbeams* (Bristol: Adam Hilger).

ZIRKLE, R. E. and BLOOM, W., 1953, Irradiation of parts of cells. *Science*, **117,** 487–493.